

# OPTIC DISC IMAGING IN PERIMETRICALLY NORMAL EYES OF GLAUCOMA PATIENTS WITH UNILATERAL FIELD LOSS

BY **Joseph Caprioli MD**,\* Kouros Nouri-Mahdavi MD, Simon K. Law MD PharmD, AND Federico Badalà, MD

## ABSTRACT

*Purpose:* To compare the ability of optic disc and retinal nerve fiber layer (RNFL) imaging to discriminate perimetrically unaffected eyes of glaucoma patients from normal eyes.

*Methods:* Forty-six primary open-angle glaucoma patients with glaucomatous visual field loss with achromatic perimetry in one eye and a normal visual field in the fellow eye and 46 normal controls were selected. Receiver operator characteristic (ROC) curves and sensitivities at fixed specificities were used to compare the performance of StratusOCT (Fast RNFL algorithm), GDx-VCC, HRT II, and clinical evaluation of optic disc photographs to distinguish perimetrically unaffected eyes of glaucoma patients from normal eyes.

*Results:* The parameters with the largest area under the ROC curves (AUC) were as follows: inferior average RNFL thickness ( $0.92 \pm 0.03$ ) for StratusOCT; linear cup-to-disc ratio ( $0.82 \pm 0.05$ ) for HRT II; and nerve fiber layer index ( $0.69 \pm 0.06$ ) for GDx-VCC. Clinical evaluation of stereoscopic disc photographs resulted in AUCs ranging between 0.80 and 0.85. The *P* values for pairwise comparisons of the AUCs of OCT's best parameter with those of HRT, GDx, and disc photographs were .06, < .001, and .17, respectively. The sensitivities at 95% specificity for the best parameters from StratusOCT (inferior average), HRT II (cup volume), GDx-VCC (temporal-superior-nasal-inferior-temporal average), and clinical evaluation of disc photographs were 61%, 39%, 37%, and 28%, respectively. OCT identified more perimetrically normal glaucomatous eyes as having abnormalities, compared to normals, than did HRT (*P* = .001), GDx (*P* = .001), or clinical evaluation of disc photographs (*P* < .001).

*Conclusion:* Optical coherence tomography (StratusOCT) may detect evidence of glaucomatous damage earlier than other imaging techniques and clinical evaluation of optic disc photographs in perimetrically unaffected eyes of primary open-angle glaucoma patients.

*Trans Am Ophthalmol Soc 2006;104:202-211*

## INTRODUCTION

The optic disc and the retinal nerve fiber layer undergo structural changes in glaucoma that often precede the appearance of visual field defects with standard perimetry.<sup>1-6</sup> Recognition of these morphological changes is important if an early diagnosis of the disease is desired. Recently, techniques of optic disc and retinal nerve fiber layer imaging have advanced and their abilities to detect anatomical changes in preperimetric glaucoma have been reported.<sup>7-15</sup> Perimetrically unaffected eyes of glaucoma patients have been found to be at high risk for developing visual field abnormalities.<sup>16-20</sup> In addition, fellow eyes of glaucoma patients with unilateral field defects have thinner neuroretinal rim and retinal nerve fiber layer compared to healthy subjects.<sup>7,21,22</sup> Studies comparing optical coherence tomography, confocal scanning laser ophthalmoscopy, scanning laser polarimetry, and clinical evaluation of the optic disc in perimetric glaucoma failed to detect significant differences among imaging methods.<sup>23</sup> The purpose of this study is to compare the above techniques in eyes at high risk for developing visual field loss from glaucoma.

## METHODS

This study was approved by the Institutional Review Board of the University of California Los Angeles (UCLA) and adhered to the tenets of the Declaration of Helsinki; informed consent was obtained from each subject. The authors reviewed the clinical database of the Glaucoma Division at Jules Stein Eye Institute (UCLA) for patients who underwent visual field testing and optic disc imaging with optical coherence tomography (StratusOCT), scanning laser ophthalmoscopy (HRT II), scanning laser polarimetry (GDx-VCC), and stereoscopic optic disc photographs at the same visit between April 2003 and April 2005. Patients with primary open-angle glaucoma, visual field defects on standard achromatic perimetry in one eye, and a normal visual field in the fellow eye were selected. To be eligible, the perimetrically unaffected eyes were required to have a visual acuity  $\geq 20/40$ , refractive error  $\leq 5$  D (spherical equivalent), and no history of other ocular diseases. Forty-six glaucoma patients and 46 normal eyes of 92 subjects older than 40 years of age were included in this cross-sectional observational study. Normal subjects were recruited from among staff, patients' spouses, and volunteers; none were patients. Normal subjects had a normal eye examination, intraocular pressure less than 21 mm Hg in both eyes, no history of ocular surgery or trauma, visual acuity  $\geq 20/40$ , refractive error  $\leq 5$  D (spherical equivalent), and a normal Humphrey 24-2 visual field.

From the Jules Stein Eye Institute, Los Angeles, California. Supported by an unrestricted grant from Research to Prevent Blindness, Inc, New York, New York; Fight for Sight; Allergan Inc; and grant RO1 EY12738 from the National Institutes of Health. This study was performed at the Glaucoma Division of the Jules Stein Eye Institute. The authors disclose no financial interests in this article.

\*Presenter.

**Bold** type indicates **AS** member.

## VISUAL FIELD CRITERIA

All patients had a 24-2 full threshold or Swedish interactive threshold algorithm (SITA) automated visual field. Only reliable fields with a fixation loss rate  $\leq 33\%$  and false-positive and false-negative rates  $\leq 20\%$  were included. To be eligible, glaucoma patients were required to have a glaucomatous visual field defect, defined as presence of a glaucoma hemifield test (GHT) outside normal limits and a pattern standard deviation (PSD) with  $P < .05$  in the worse eye and a normal GHT and PSD  $P$  value  $> .05$  in the fellow eye.

## IMAGING METHODS

### Optical Coherence Tomography (Stratus OCT)

The fast retinal nerve fiber layer (RNFL) thickness algorithm of Stratus OCT was used to evaluate peripapillary RNFL thickness. The instrument acquires three images, each consisting of 256 A-scans along a circular ring (3.4 mm in diameter) around the optic disc. The data were exported to a desktop computer, and the three measurements were averaged. The parameters calculated by the OCT software (version 3.1) and evaluated in this study were as follows: average RNFL thickness; RNFL thickness in each quadrant (superior, inferior, nasal, and temporal); RNFL thickness in each of the 12 clock-hour sectors; thickest points in the superior and inferior quadrants (Smax and Imax, respectively); the difference between the thickest and thinnest measured points (Max – Min); and the following ratios: Imax/Smax, Smax/Imax, Smax/temporal average RNFL thickness (Tavg), Imax/Tavg, Smax/nasal average RNFL thickness (Navg). The OCT software compares each parameter with a normative database and classifies them as follows: normal (within the upper 95% of control eyes), borderline (observed between 5% and 1% of normal eyes), and abnormal (observed in less than 1% of the control eyes).

### Confocal Scanning Laser Ophthalmoscopy (HRT II)

Confocal scanning laser ophthalmoscopy (Heidelberg Retina Tomograph, HRT II, Heidelberg Engineering GmbH, Heidelberg, Germany) was performed in each patient as follows. Three 15° topographic images (obtained in the same sitting) were aligned and averaged to obtain a mean topography. An experienced ophthalmic photographer outlined the optic disc margin. One of the authors (F.B.) reviewed all the images and redrew the optic disc contour line when the contour line did not coincide with the disc border, defined as the inner edge of the scleral ring of Elshnig. The following HRT parameters were examined in this study: disc area, cup area, rim area, cup-to-disc area ratio, rim-to-disc area ratio, cup volume, rim volume, mean cup depth, maximum cup depth, height variation contour, cup shape measure, mean RNFL thickness, RNFL cross-sectional area, horizontal and vertical cup-to-disc ratios, linear cup-to-disc ratio, and the FSM (Mikelberg<sup>24</sup>) and RB (Bathija<sup>25</sup>) discriminant functions. In addition, the Moorfields regression analysis of the HRT II software compares the rim area (globally and sectorally) with a normative database that takes into account the patient's age and disc area and classifies it as follows: within normal limits (within the upper 95% confidence limits for control eyes); borderline (observed among the lower 95% and 99.9% of normal eyes); and outside normal limits (observed in less than the lower 0.1% of normal patients).

### Scanning Laser Polarimeter (GDx-VCC)

The scanning laser polarimeter with variable corneal compensation (GDx-VCC; Laser Diagnostic Technologies, San Diego, California; software version 5.2.3) was used to measure peripapillary RNFL. The RNFL thickness is measured along the temporal-superior-nasal-inferior-temporal (TSINT) portions of a calculation circle (0.4-mm width, outer diameter 3.2 mm, and inner diameter 2.4 mm) centered on the optic nerve head. This circular arc is divided into superior (120°), inferior (120°), nasal (50°), and temporal (70°) quadrants. The parameters calculated by the GDx software shown on the printout and evaluated in this study are as follows: TSNIT average, superior average, inferior average, TSNIT standard deviation (TSNIT SD), and intereye symmetry. TSNIT average is the average RNFL thickness along the calculation circle. Superior and inferior averages are the average RNFL thicknesses in the superior and inferior quadrants of the calculation circle, respectively. TSNIT SD is the standard deviation of RNFL measurements along the calculation circle. Intereye symmetry is a measure of the correlation of corresponding points of TSNIT data for the right and left eyes.

Each of the above parameters is compared with a normative database, and the probability of abnormality is shown in a color-coded table.  $P$  values were classified as follows: more than 5% (displayed in green) as normal, between 1% and 5% (displayed in blue and purple) as borderline, and less than 1% (displayed in yellow and red) as abnormal. Based on the entire RNFL thickness measurements, an indicator called nerve fiber indicator (NFI) is calculated with a neural network algorithm. It varies between 0 and 100, with 100 indicating the highest likelihood of glaucoma. For categorization purposes, NFI  $\leq 30$  was considered as normal, 31 to 50 as borderline, and  $> 50$  as abnormal.<sup>26</sup> Raw data were exported from the GDx to a desktop computer and used for further analysis.

### Optical Disc Stereophotographs

Stereophotographs of the optic disc (ODPs) were obtained sequentially in each subject with a fundus camera (Fundus Flash III; Carl Zeiss, Oberkochen, Germany). The optic disc photographs were reviewed by three experienced observers (J.C., K.N.-M., S.K.L.) masked to patients' identities and diagnoses. Fifty additional ODPs belonging to normal subjects, subjects suspected of having glaucoma, and subjects with glaucoma (early to advanced optic disc damage) were added to the ODP pool to minimize evaluation bias. One eye from each subject was evaluated to reduce bias resulting from optic disc asymmetry. Each ODP was graded as follows: 1, normal; 2, probably normal; 3, undetermined; 4, probable glaucoma; and 5, glaucoma. A summary score was calculated by summing the scores assigned by the three observers.

**Statistical Analyses**

The Wilk-Shapiro test was used to evaluate the distribution of numeric variables. Normally distributed variables were compared with the independent-sample *t* test. Numeric variables that were not normally distributed were compared with the Mann-Whitney *U* test. Receiver operating characteristic (ROC) curves were used to evaluate performance of each imaging method for discriminating perimetrically unaffected eyes of glaucoma patients from normal eyes. Areas under the ROC curves (AUCs) were compared with the software Stata (version 8.2, Stata Corporation, College Station, Texas). Specificity cutoffs of 80% and 95% were used to compare sensitivity of the best parameters from each imaging device. Sensitivities at fixed specificities were compared with the McNemar test.

**RESULTS**

The study sample included 46 perimetrically unaffected eyes of primary open-angle glaucoma patients and 46 eyes from 46 normal subjects (Table 1). The average mean deviation ( $\pm$  SD) in the glaucoma and normal groups was  $-0.8 \pm 1.5$  and  $0.1 \pm 1.2$  dB, respectively (Mann-Whitney test,  $P < .01$ ). The average pattern standard deviation was also significantly different in the two groups ( $1.7 \pm 0.5$  dB in the glaucoma group and  $1.4 \pm 0.2$  in the normal group; Mann-Whitney test,  $P = .02$ ). All images had good centration and focusing; however, eight glaucoma patients had GDx-VCC image quality score of  $<8$ , one patient had an HRT II mean topography standard deviation  $>50\mu$ , and three OCT images were not perfectly centered (all OCT images had noise-to-signal ratio  $> 25$  dB). No image was discarded from the study.

**TABLE 1. DEMOGRAPHIC CHARACTERISTICS OF THE STUDY SAMPLE\***

VARIABLE	NORMAL GROUP	GLAUCOMA GROUP (PERIMETRICALLY UNAFFECTED EYES)	P VALUE
No. of eyes	46 (50%)	46 (50%)	
Age (mean $\pm$ SD, years)	58.9 $\pm$ 6.8	62.7 $\pm$ 11.7	.07 <sup>†</sup>
Gender (F/M)	26 (57%)/20 (43%)	23 (50%)/23 (50%)	.53 <sup>‡</sup>
Ethnicity			.07 <sup>‡</sup>
Caucasian	25 (54%)	31 (67%)	
African American	1 (2%)	5 (11%)	
Hispanic	9 (20%)	3 (7%)	
Asian	11 (24%)	7 (15%)	
IOP (mm Hg, mean $\pm$ SD)	14.0 $\pm$ 2.9	14.5 $\pm$ 3.4	.99 <sup>†</sup>
Mean deviation (dB, mean $\pm$ SD)	0.1 $\pm$ 1.2	-0.8 $\pm$ 1.5	< .01 <sup>§</sup>
Pattern standard deviation (dB, mean $\pm$ SD)	1.4 $\pm$ 0.2	1.7 $\pm$ 0.5	.02 <sup>§</sup>
Spherical equivalent (D)	-0.4 $\pm$ 1.7	-0.1 $\pm$ 2.4	.99 <sup>§</sup>

\*The study samples consisted of perimetrically normal fellow eyes of primary open-angle glaucoma patients with unilateral visual field loss on standard automated perimetry, and a group of normal control subjects. Each individual underwent optic disc imaging with StratusOCT, HRT II, GDx-VCC, and optic disc stereophotography.

<sup>†</sup>Independent-sample *t* test.

<sup>‡</sup>Chi-square test.

<sup>§</sup>Mann-Whitney test.

**OPTICAL COHERENCE TOMOGRAPHY (STRATUSOCT)**

The StratusOCT parameters in perimetrically unaffected and normal eyes, AUCs, and sensitivities at  $\geq 80\%$  and  $\geq 95\%$  specificities are presented in Table 2. The three parameters with the largest AUC ( $\pm$  SE) were inferior average RNFL thickness ( $0.92 \pm 0.03$ ), superior average RNFL thickness ( $0.86 \pm 0.04$ ), and inferior quadrant RNFL thickness ( $0.77 \pm 0.05$ ). The RNFL thickness in the inferior quadrant, inferior average RNFL thickness, and average RNFL thickness had the highest diagnostic precisions. When the analyses were repeated after exclusion of the three eyes with reduced quality images, no significant change in diagnostic accuracies was detected.

**TABLE 2. STRATUSOCT PARAMETERS IN PERIMETRICALLY UNAFFECTED EYES OF GLAUCOMA PATIENTS AND NORMAL EYES: RETINAL NERVE FIBER LAYER THICKNESSES (μM), AREAS UNDER THE RECEIVER OPERATING CHARACTERISTIC (ROC) CURVES, AND SENSITIVITIES AT FIXED SPECIFICITIES**

PARAMETER	GLAUCOMA PATIENTS PERIMETRICALLY UNAFFECTED EYES (MEAN ± SD)	NORMAL (MEAN ± SD)	P VALUE	ROC ± SE	SENSITIVITY AT ≥ 80% SPECIFICITY ± SE	SENSITIVITY AT ≥ 95% SPECIFICITY ± SE
Inferior average	85.1 ± 13.4	116.1 ± 17.8	<.001*	0.92 ± 0.03	89 ± 5%	61 ± 7%
Superior average	88.6 ± 12.8	112.7 ± 18.9	<.001 <sup>†</sup>	0.86 ± 0.04	83 ± 6%	44 ± 7%
Inferior quadrant	107.9 ± 19.7	128.0 ± 17.5	<.001*	0.77 ± 0.05	54 ± 7%	41 ± 7%
Average thickness	86.9 ± 12.1	98.0 ± 11.2	<.001*	0.76 ± 0.05	59 ± 7%	39 ± 7%
Sector 6	112.2 ± 26.3	137.5 ± 24.7	<.001*	0.76 ± 0.05	54 ± 7%	37 ± 7%
Superior quadrant	105.0 ± 18.1	122.1 ± 18.6	<.001*	0.75 ± 0.05	57 ± 7%	28 ± 7%
Inferior maximum	142.5 ± 25.4	163.9 ± 21.0	<.001*	0.75 ± 0.05	59 ± 7%	30 ± 7%
Sector 1	90.0 ± 21.8	112.0 ± 23.7	<.001*	0.74 ± 0.05	46 ± 7%	26 ± 6%
Sector 7	123.5 ± 26.0	141.9 ± 20.9	<.001*	0.72 ± 0.05	61 ± 7%	17 ± 6%
Sector 12	104.5 ± 25.4	125.4 ± 23.4	<.001*	0.72 ± 0.05	46 ± 7%	24 ± 6%
Superior maximum	139.0 ± 22.7	153.9 ± 19.0	.001*	0.72 ± 0.05	52 ± 7%	24 ± 6%
Sector 5	87.9 ± 22.7	104.4 ± 20.6	<.001*	0.71 ± 0.05	57 ± 7%	35 ± 7%
Max-Min	113.1 ± 24.7	126.6 ± 16.9	<.001 <sup>†</sup>	0.71 ± 0.05	52 ± 7%	39 ± 7%
Sector 2	73.8 ± 21.3	89.4 ± 21.3	.001*	0.71 ± 0.05	48 ± 7%	26 ± 6%
Smax/Tavg	2.1 ± 0.48	2.22 ± 0.42	.005 <sup>†</sup>	0.67 ± 0.06	48 ± 7%	22 ± 6%
Nasal quadrant	62.4 ± 15.8	70.8 ± 16.1	.013*	0.66 ± 0.06	50 ± 7%	22 ± 6%
Imax/Tavg	2.1 ± 0.56	2.38 ± 0.53	.014 <sup>†</sup>	0.65 ± 0.06	35 ± 7%	24 ± 6%
Sector 11	120.6 ± 23.4	128.8 ± 25.1	.107*	0.63 ± 0.06	48 ± 7%	02 ± 2%
Sector 4	60.8 ± 17.2	66.5 ± 18.1	.095 <sup>†</sup>	0.60 ± 0.06	30 ± 7%	11 ± 2%
Sector 3	53.2 ± 15.2	56.8 ± 14.4	.244*	0.55 ± 0.06	28 ± 7%	15 ± 5%
Smax/Imax	1.0 ± 0.21	0.95 ± 0.13	.380 <sup>†</sup>	0.55 ± 0.06	35 ± 7%	20 ± 6%
Imax/Smax	1.0 ± 0.21	1.08 ± 0.16	.389*	0.55 ± 0.06	35 ± 7%	20 ± 6%
Sector 8	75.6 ± 21.6	77.0 ± 17.1	.725*	0.55 ± 0.06	30 ± 7%	07 ± 4%
Temporal quadrant	72.1 ± 18.8	71.2 ± 13.5	.799*	0.53 ± 0.06	33 ± 7%	04 ± 3%
Sector 9	56.4 ± 15.8	55.2 ± 11.0	.821 <sup>†</sup>	0.51 ± 0.06	24 ± 6%	04 ± 3%
Sector 10	85.0 ± 23.8	81.7 ± 18.4	.901*	0.51 ± 0.06	28 ± 7%	02 ± 2%
Smax/Navg	2.4 ± 0.88	2.26 ± 0.48	1.00 <sup>†</sup>	0.50 ± 0.06	15 ± 5%	02 ± 2%

Imax = inferior quadrant maximum thickness; Max-Min = Maximum thickness – minimum thickness; Navg = nasal quadrant average thickness; Smax = superior quadrant maximum thickness; Tavg = temporal quadrant average thickness.

\*Independent-sample *t* test.

<sup>†</sup>Mann-Whitney test.

**SCANNING LASER OPHTHALMOSCOPY (HRT II)**

The HRT II parameters in perimetrically unaffected and normal eyes, AUCs, and sensitivities at ≥80% and ≥95% specificities are presented in Table 3. The three parameters with the largest AUC (± SE) were linear cup-to-disc ratio (0.82 ± 0.05), cup-to-disc area ratio (0.82 ± 0.05), and cup volume (0.80 ± 0.05). Removing the eye with a reduced-quality image did not change the results.

**TABLE 3. HRT II PARAMETERS AND DISCRIMINANT FUNCTIONS IN PERIMETRICALLY UNAFFECTED EYES OF GLAUCOMA PATIENTS AND NORMAL EYES: AREAS UNDER THE RECEIVER OPERATING CHARACTERISTIC (ROC) CURVES AND SENSITIVITIES AT FIXED SPECIFICITIES**

PARAMETER	GLAUCOMA PERIMETRICALLY UNAFFECTED EYES (MEAN ± SD)	NORMAL (MEAN ± SD)	P VALUE	ROC ± SE	SENSITIVITY AT ≥ 80% SPECIFICITY ± SE	SENSITIVITY AT ≥ 95% SPECIFICITY ± SE
Linear cup-to-disc ratio	0.59 ± 0.13	0.41 ± 0.17	<.001 <sup>†</sup>	0.82 ± 0.05	76 ± 6%	28 ± 7%
Cup-to-disc area ratio	0.37 ± 0.14	0.20 ± 0.13	<.001*	0.82 ± 0.05	76 ± 6%	28 ± 7%
Cup volume (mm <sup>3</sup> )	0.26 ± 0.24	0.09 ± 0.14	<.001 <sup>†</sup>	0.80 ± 0.05	67 ± 7%	39 ± 7%
Cup area (mm <sup>2</sup> )	0.82 ± 0.45	0.40 ± 0.33	<.001 <sup>†</sup>	0.79 ± 0.05	65 ± 7%	28 ± 7%
Mean cup depth (mm)	0.30 ± 0.12	0.19 ± 0.09	<.001 <sup>†</sup>	0.78 ± 0.05	63 ± 7%	37 ± 7%
FSM discriminant function value	0.41 ± 1.66	1.96 ± 1.73	<.001*	0.76 ± 0.05	63 ± 7%	28 ± 7%
Maximum cup depth (mm)	0.75 ± 0.29	0.54 ± 0.20	<.001 <sup>†</sup>	0.73 ± 0.05	52 ± 7%	39 ± 7%
Cup shape measure	-0.14 ± 0.07	-0.20 ± 0.07	<.001*	0.72 ± 0.05	57 ± 7%	17 ± 6%
RB discriminant function value	0.94 ± 0.83	1.54 ± 0.64	<.001*	0.72 ± 0.05	63 ± 7%	28 ± 7%
Rim volume (mm <sup>3</sup> )	0.32 ± 0.13	0.43 ± 0.14	<.001*	0.72 ± 0.05	54 ± 7%	26 ± 6%
Rim area (mm <sup>2</sup> )	1.31 ± 0.28	1.53 ± 0.33	<.001 <sup>†</sup>	0.71 ± 0.05	46 ± 7%	09 ± 4%
Mean RNFL thickness (mm)	0.22 ± 0.07	0.27 ± 0.05	.001 <sup>†</sup>	0.71 ± 0.06	63 ± 7%	22 ± 6%
RNFL cross sectional area (mm <sup>2</sup> )	1.13 ± 0.37	1.33 ± 0.32	.008*	0.65 ± 0.06	44 ± 7%	17 ± 6%
Disc area (mm <sup>2</sup> )	2.13 ± 0.48	1.93 ± 0.40	.043 <sup>†</sup>	0.62 ± 0.06	37 ± 7%	13 ± 5%
Height variation contour (mm)	0.37 ± 0.10	0.41 ± 0.10	.055*	0.60 ± 0.06	46 ± 7%	09 ± 4%
Reference height (mm)	0.34 ± 0.10	0.35 ± 0.12	.592*	0.53 ± 0.06	20 ± 6%	02 ± 2%

FSM = Mikelberg discriminant function; RB = Bathija discriminant function; RNF = retinal nerve fiber layer.

\*Independent-sample *t* test.

<sup>†</sup>Mann-Whitney test.

**SCANNING LASER POLARIMETRY (GDx-VCC)**

Table 4 presents GDx-VCC parameters in perimetrically unaffected and normal eyes, AUCs, and sensitivities at ≥80% and ≥95% specificities. The three parameters with the largest AUC (± SE) were NFI (0.69 ± 0.06), TSNIT SD (0.66 ± 0.06), and superior average (0.65 ± 0.06). After excluding eight eyes with questionable images, the diagnostic accuracy for all parameters slightly improved as follows (AUCs): NFI (0.73 ± 0.06); TSNIT SD (0.69 ± 0.06), and superior average (0.68 ± 0.06).

**OPTIC DISC STEREOPHOTOGRAPHS**

The agreement among observers was fair to moderate. Observer 1 and observer 2 agreed in 68% of the cases (κ = 0.49; 95% CI, 0.33-0.64), whereas observer 1 and observer 3 agreed in 57% of the cases (κ = 0.35; 95% CI, 0.20-0.51). Agreement between observer 2 and observer 3 was observed 56% of the time (κ = 0.35; 95% CI, 0.21-0.51). Table 5 shows the results of qualitative evaluation of optic disc photographs by three experienced observers. AUCs ranged from 0.80 to 0.83 for individual observers. The AUC obtained using the cumulative score from the three observers was 0.85; sensitivities (± SE) at ≥80% and ≥95% specificities were 0.70 ± 6% and 0.28 ± 7%.

**COMPARISON OF IMAGING METHODS**

The ROC curves for the best parameters of the three devices and for clinical evaluation of disc photographs (cumulative score) were compared. The AUC for OCT inferior average thickness (0.92 ± 0.03) was significantly better than that of NFI (0.69 ± 0.06) from GDx (*P* < .001). Excluding eyes with questionable images did not change this result. Optical coherence tomography's inferior average thickness (0.92 ± 0.03) also performed better than linear cup-to-disc ratio (0.82 ± 0.05) from HRT and clinical evaluation of optic disc photographs (0.85 ± 0.04), but the differences for the last two comparisons were not statistically significant (*P* = .06 and .17, respectively). The corresponding ROC curves are shown in Figure 1. Tables 6 and 7 show the *P* values for comparison of sensitivities at ≥80% and 95% specificities for the best parameter from each device and for evaluation of disc photographs (cumulative score). When parameters with the highest sensitivity at ≥80% specificity were compared, OCT's inferior average RNFL thickness (89%) showed more abnormalities than HRT's linear cup-to-disc ratio (76%; *P* < .03) and clinical evaluation of disc photographs (70%; *P* = .004). HRT's linear cup-to-disc ratio showed more abnormalities than GDx's NFI (52%; *P* < .001). Likewise, the sensitivity of clinical evaluation of disc photographs was higher than GDx's NFI (*P* = .008). At a specificity of 95%, OCT also was significantly more affected than all other imaging methods.

**TABLE 4. GDx-VCC PARAMETERS IN PERIMETRICALLY UNAFFECTED EYES OF GLAUCOMA PATIENTS AND NORMAL EYES: RETINAL NERVE FIBER LAYER THICKNESSES ( $\mu\text{M}$ ), AREAS UNDER THE RECEIVER OPERATING CHARACTERISTIC (ROC) CURVES, AND SENSITIVITIES AT FIXED SPECIFICITIES**

PARAMETER	GLAUCOMA PATIENTS PERIMETRICALLY UNAFFECTED EYES (MEAN $\pm$ SD)	NORMAL (MEAN $\pm$ SD)	P VALUE	ROC $\pm$ SE	SENSITIVITY AT $\geq 80\%$ SPECIFICITY $\pm$ SE	SENSITIVITY AT $\geq 95\%$ SPECIFICITY $\pm$ SE
NFI	27.7 $\pm$ 14.3	19.2 $\pm$ 8.2	.002 <sup>†</sup>	0.69 $\pm$ 0.06	52 $\pm$ 7%	26 $\pm$ 6%
TSNIT SD	18.3 $\pm$ 5.3	21.3 $\pm$ 4.7	.004*	0.66 $\pm$ 0.06	41 $\pm$ 7%	17 $\pm$ 6%
Superior average	61.5 $\pm$ 9.8	65.9 $\pm$ 7.9	.019*	0.65 $\pm$ 0.06	48 $\pm$ 7%	17 $\pm$ 6%
Inferior average	60.2 $\pm$ 12.8	64.8 $\pm$ 8.7	.049*	0.62 $\pm$ 0.06	50 $\pm$ 7%	20 $\pm$ 6%
TSNIT average	53.3 $\pm$ 8.2	55.1 $\pm$ 5.9	.208*	0.57 $\pm$ 0.06	46 $\pm$ 7%	37 $\pm$ 7%
Intereye symmetry	1.0 $\pm$ 0.2	1.0 $\pm$ 0.1	.897 <sup>†</sup>	0.51 $\pm$ 0.06	35 $\pm$ 7%	20 $\pm$ 6%

\*Independent sample *t* test.

<sup>†</sup>Mann-Whitney test.

NFI = nerve fiber index; SD = standard deviation; TSNIT = temporal-superior-nasal-inferior-temporal.

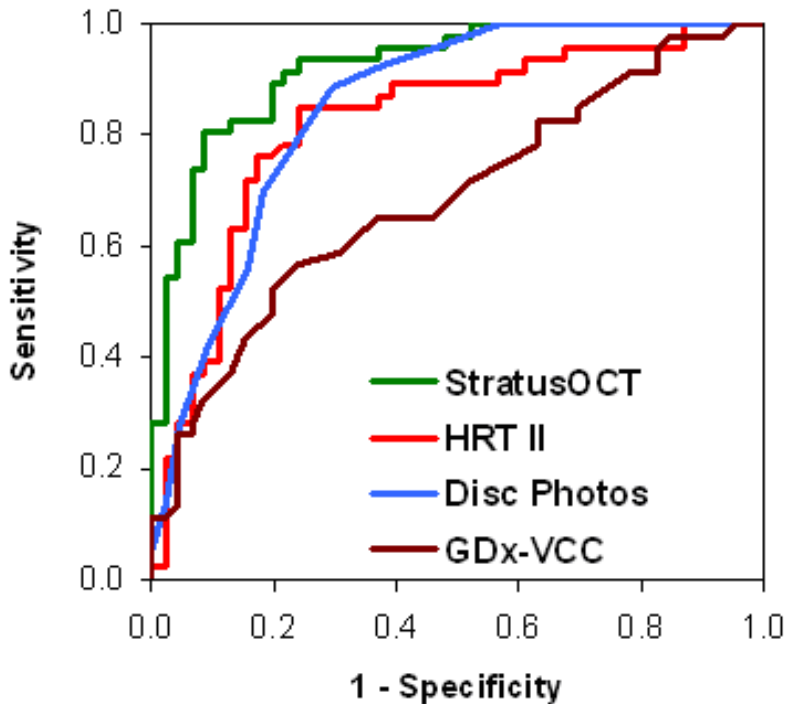


**FIGURE 1**

Comparison of the receiver operator characteristic (ROC) curves for the best parameters from StratusOCT, GDx-VCC, HRT II, and clinical evaluation of optic disc photographs. Areas under the ROC curves were as follows: 0.92 for inferior average thickness from OCT, 0.85 for disc photographs evaluation (cumulative score), 0.82 for linear cup-to-disk ratio from HRT, and 0.69 for nerve fiber layer index from GDx.

**TABLE 5. AREAS UNDER THE RECEIVER OPERATING CHARACTERISTIC (ROC) CURVES FOR QUALITATIVE EVALUATION OF OPTIC DISC STEREOPHOTOGRAPHS**

DISC PHOTOGRAPH OBSERVER	ROC ± SE
Observer 1	0.80 ± 0.05
Observer 2	0.83 ± 0.04
Observer 3	0.81 ± 0.05
Cumulative score	0.85 ± 0.04

**TABLE 6. P VALUES FOR COMPARISON OF SENSITIVITIES AT ≥80% SPECIFICITIES BETWEEN THE BEST PARAMETERS OF STRATUSOCT, HRT II, GDx-VCC, AND CLINICAL EVALUATION OF DISC PHOTOGRAPHS (CUMULATIVE SCORE)\***

IMAGING TECHNIQUE (SENSITIVITY AT ≥80% SPECIFICITY)	P VALUES FOR COMPARISONS OF SENSITIVITIES AT ≥80% SPECIFICITIES		
	STRATUSOCT	HRT II	GDx-VCC
StratusOCT (89 ± 5%)	–	–	–
HRT II (76 ± 6%)	.03	–	–
GDx-VCC (52 ± 7%)	< .001	.001	–
Disc photographs (70 ± 6%)	.004	.25	.008

\*The McNemar’s test was used for all pairwise comparisons.

**TABLE 7. P VALUES FOR COMPARISONS OF SENSITIVITIES AT ≥95% SPECIFICITIES BETWEEN THE BEST PARAMETERS OF STRATUSOCT, HRT II, GDx-VCC, AND CLINICAL EVALUATION OF DISC PHOTOGRAPHS (CUMULATIVE SCORE)\***

IMAGING TECHNIQUE (SENSITIVITY AT ≥95% SPECIFICITY)	P VALUES FOR COMPARISONS OF SENSITIVITIES AT ≥95% SPECIFICITIES		
	STRATUSOCT	HRT II	GDx-VCC
StratusOCT (61 ± 7%)	–	–	–
HRT II (39 ± 7%)	.002	–	–
GDx-VCC (37 ± 7%)	.001	1.0	–
Disc photographs (28 ± 7%)	< .001	.06	.125

\*The McNemar’s test was used for all pairwise comparisons.

## DISCUSSION

This is the first study to compare optical coherence tomography (StratusOCT), confocal scanning laser ophthalmoscopy (HRT II), scanning laser polarimetry (GDx-VCC), and clinical evaluation of the optic disc in preperimetric glaucoma (perimetrically unaffected eyes of open-angle glaucoma patients with unilateral visual field loss). StratusOCT discriminates perimetrically normal fellow eyes of patients with primary open-angle glaucoma from normal controls better than HRT II, GDx-VCC, or clinical evaluation of the optic nerve by experienced observers.

The perimetrically unaffected eyes of primary open-angle glaucoma patients with unilateral field loss are being used here to

represent a group of patients with very early, preperimetric glaucoma. Primary open-angle glaucoma is predominantly a bilateral disease, and “preperimetric” eyes are at high subsequent risk for developing demonstrable abnormalities.<sup>16-22,27</sup> Many studies have reported the ability of different imaging methods to detect glaucomatous damage before visual field defects become manifest. Medeiros and colleagues<sup>10</sup> recently reported high diagnostic accuracy for GDx-VCC in patients with progressive changes of the optic disc over time but without visual field abnormalities. The NFI discriminated preperimetric glaucoma patients from healthy subjects (AUC = 0.89). In addition, the GDx-VCC seemed to recognize early signs of glaucomatous damage in ocular hypertensive eyes. The NFI showed more advanced damage in patients with ocular hypertension and thinner corneas compared to patients with ocular hypertension and thicker corneas and the normal control group.<sup>6</sup> Moreover, thinner GDx-VCC NFI measurements at baseline were found to be predictive of future visual field loss in a longitudinal study by Mohammadi and associates.<sup>8</sup>

Optical coherence tomography (OCT 2000 and StratusOCT) has been shown to detect a thinner RNFL in the inferior quadrant of ocular hypertensive patients compared to normal subjects.<sup>11,12</sup> In a study by Mok and associates,<sup>28</sup> eyes with abnormal short-wavelength automated perimetry (SWAP) and normal achromatic visual fields had lower RNFL thicknesses in the superotemporal and inferotemporal sectors compared to normal controls. Other investigators have reported a good correlation between SWAP defects and RNFL thicknesses measured with OCT.<sup>29</sup> Kanamori and colleagues<sup>30</sup> evaluated the diagnostic accuracy of OCT 2000 in subjects with suspected glaucoma (normal achromatic visual fields and glaucomatous optic discs). The parameters with the largest AUCs were the RNFL thickness in the inferior quadrant, sector 6, and overall average RNFL thickness. In a longitudinal study of glaucoma patients and glaucoma suspects, an OCT prototype was more likely to identify progression than standard perimetry.<sup>13</sup>

Confocal scanning laser ophthalmoscopy predicted future field loss in eyes with suspected glaucoma.<sup>14</sup> An abnormal Moorfields regression analysis at baseline was associated with a 54% increased risk of developing a confirmed field defect during 4.5 years of follow-up. In the same study, glaucomatous-appearing optic discs on stereophotography had a 100% greater chance of visual field loss. Ugurlu and colleagues<sup>15</sup> found that HRT was able to detect structural abnormalities in ocular hypertensive patients with normal achromatic perimetry and abnormal SWAP. Iester and associates<sup>31</sup> could not distinguish ocular hypertensive eyes from a normal control group with HRT I.

In perimetric glaucoma, the diagnostic precision of StratusOCT, HRT II, GDx-VCC, and clinical evaluation of disc photographs is very high, and previous studies have failed to detect clinically significant differences among the methods. However, in a recent investigation, Medeiros and associates<sup>23</sup> reported OCT (inferior thickness) and GDx (NFI) sensitivity at  $\geq 80\%$  specificity to be significantly better than HRT (Mikelberg function). The existing evidence that optic nerve and nerve fiber layer imaging techniques can detect glaucomatous damage before visual field loss makes it relevant to compare them in eyes with preperimetric glaucoma. This study evaluated the diagnostic precision of each method with areas under the ROC curves, and sensitivities at fixed specificities. The larger the area under the ROC curve, the higher the diagnostic precision.

For StratusOCT, the inferior and superior average RNFL thicknesses were found to have the largest AUCs (0.92 and 0.86, respectively) and sensitivities at 80% and 95% specificities. The StratusOCT provides diagnostic categorization after comparing each parameter with a normative database. For HRT II parameters, linear cup-to-disc ratio were found to have the largest area under the ROC curve (0.82). The difference from OCT’s inferior average thickness may be clinically relevant but was only of borderline statistical significance ( $P = .06$ ). GDx-VCC diagnostic precision in this study was lower than has been previously reported. In our study sample, eight of the glaucoma patients had questionable image quality (quality factor  $< 8$ ). When these eyes were removed from the analysis, diagnostic performance did not significantly improve. The ability to acquire good-quality images is an important variable to consider when evaluating the diagnostic performance of an instrument. Among the GDx-VCC parameters, the NFI had the largest area under the ROC curve (0.69, and 0.73 with no questionable quality images), which was significantly less than the AUC from the OCT inferior average.

Qualitative evaluation of optic disc stereophotographs by experienced observers performed less well than the StratusOCT. The AUC for the cumulative score (0.85), which reflected the opinion of three glaucoma specialists, was smaller than that of OCT. At specificities  $\geq 80\%$  and  $\geq 95\%$ , OCT was significantly better than all other imaging methods.

In conclusion, the present study demonstrates that optical coherence tomography (StratusOCT) discriminates the perimetrically unaffected fellow eyes of patients with primary open-angle glaucoma from normal controls more effectively than other imaging techniques. The inferior and superior average RNFL thicknesses were the parameters that best distinguished these eyes from normal eyes. These findings suggest, but do not prove, that such measurements may identify very early glaucomatous damage more effectively than confocal laser ophthalmoscopy, NFL polarimetry, or “expert” optic disc evaluation. These preliminary findings will require confirmation by external validation with long-term longitudinal follow-up to determine the incidence of subsequent visual field loss. Historically, these eyes are at high risk for subsequent demonstrable glaucomatous damage. This report suggests that very early structural glaucomatous damage may be more effectively identified with NFL imaging rather than with clinical evaluation of optic disc stereophotographs.

## REFERENCES

1. Johnson CA, Sample PA, Zangwill LM, et al. Structure and function evaluation (SAFE): II. Comparison of optic disk and visual field characteristics. *Am J Ophthalmol* 2003;135:148-154.
2. Airaksinen PJ, Drance SM, Douglas GR, et al. Visual field and retinal nerve fiber layer comparisons in glaucoma. *Arch Ophthalmol* 1985;103:205-207.

3. Tuulonen A, Airaksinen PJ. Initial glaucomatous optic disk and retinal nerve fiber layer abnormalities and their progression. *Am J Ophthalmol* 1991;111:485-490.
4. Sommer A, Katz J, Quigley HA, et al. Clinically detectable nerve fiber atrophy precedes the onset of glaucomatous field loss. *Arch Ophthalmol* 1991;109:77-83.
5. Harwerth RS, Carter-Dawson L, Shen F, et al. Ganglion cell losses underlying visual field defects from experimental glaucoma. *Invest Ophthalmol Vis Sci* 1999;40:2242-2250.
6. Kass MA, Heuer DK, Higginbotham EJ, et al. The Ocular Hypertension Treatment Study: a randomized trial determines that topical ocular hypotensive medication delays or prevents the onset of primary open-angle glaucoma. *Arch Ophthalmol* 2002;120:701-713; discussion 829-830.
7. Reus NJ, Lemij HG. Scanning laser polarimetry of the retinal nerve fiber layer in perimetrically unaffected eyes of glaucoma patients. *Ophthalmology* 2004;111:2199-2203.
8. Mohammadi K, Bowd C, Weinreb RN, et al. Retinal nerve fiber layer thickness measurements with scanning laser polarimetry predict glaucomatous visual field loss. *Am J Ophthalmol* 2004;138:592-601.
9. Henderson PA, Medeiros FA, Zangwill LM, Weinreb RN. Relationship between central corneal thickness and retinal nerve fiber layer thickness in ocular hypertensive patients. *Ophthalmology* 2005;112:251-256.
10. Medeiros FA, Zangwill LM, Bowd C, et al. Use of progressive glaucomatous optic disk change as the reference standard for evaluation of diagnostic tests in glaucoma. *Am J Ophthalmol* 2005;139:1010-1018.
11. Choi MG, Han M, Kim YI, Lee JH. Comparison of glaucomatous parameters in normal, ocular hypertensive and glaucomatous eyes using optical coherence tomography 3000. *Korean J Ophthalmol* 2005;19:40-46.
12. Bowd C, Weinreb RN, Williams JM, Zangwill LM. The retinal nerve fiber layer thickness in ocular hypertensive, normal, and glaucomatous eyes with optical coherence tomography. *Arch Ophthalmol* 2000;118:22-26.
13. Wollstein G, Schuman JS, Price LL, et al. Optical coherence tomography longitudinal evaluation of retinal nerve fiber layer thickness in glaucoma. *Arch Ophthalmol* 2005;123:464-470.
14. Bowd C, Zangwill LM, Medeiros FA, et al. Confocal scanning laser ophthalmoscopy classifiers and stereophotograph evaluation for prediction of visual field abnormalities in glaucoma-suspect eyes. *Invest Ophthalmol Vis Sci* 2004;45:2255-2262.
15. Ugurlu S, Hoffman D, Garway-Heath DF, Caprioli J. Relationship between structural abnormalities and short-wavelength perimetric defects in eyes at risk of glaucoma. *Am J Ophthalmol* 2000;129:592-598.
16. Fontana L, Armas R, Garway-Heath DF, et al. Clinical factors influencing the visual prognosis of the fellow eyes of normal tension glaucoma patients with unilateral field loss. *Br J Ophthalmol* 1999;83:1002-1005.
17. Harbin TS Jr, Podos SM, Kolker AE, Becker B. Visual field progression in open-angle glaucoma patients presenting with monocular field loss. *Trans Sect Ophthalmol Am Acad Ophthalmol Otolaryngol* 1976;81:253-257.
18. Kass MA, Kolker AE, Becker B. Prognostic factors in glaucomatous visual field loss. *Arch Ophthalmol* 1976;94:1274-1276.
19. Susanna R, Drance SM, Douglas GR. The visual prognosis of the fellow eye in uniocular chronic open-angle glaucoma. *Br J Ophthalmol* 1978;62:327-329.
20. Chen PP, Park RJ. Visual field progression in patients with initially unilateral visual field loss from chronic open-angle glaucoma. *Ophthalmology* 2000;107:1688-1692.
21. Caprioli J, Miller JM, Sears M. Quantitative evaluation of the optic nerve head in patients with unilateral visual field loss from primary open-angle glaucoma. *Ophthalmology* 1987;94:1484-1487.
22. Zeyen TG, Raymond M, Caprioli J. Disc and field damage in patients with unilateral visual field loss from primary open-angle glaucoma. *Doc Ophthalmol* 1992;82:279-286.
23. Medeiros FA, Zangwill LM, Bowd C, Weinreb RN. Comparison of the GDx VCC scanning laser polarimeter, HRT II confocal scanning laser ophthalmoscope, and stratus OCT optical coherence tomograph for the detection of glaucoma. *Arch Ophthalmol* 2004;122:827-837.
24. Mikelberg FS, Parfitt CV, Swindale NV, et al. Ability of the Heidelberg Retina Tomograph to detect early glaucomatous visual field loss. *J Glaucoma* 1995;4:242-247.
25. Bathija R, Zangwill L, Berry CC, et al. Detection of early glaucomatous structural damage with confocal scanning laser tomography. *J Glaucoma* 1998;7:121-127.
26. GDx-VCC Operation Manual version 5.2.3. San Diego, California: Laser Diagnostic Technologies.
27. Susanna R Jr, Galvao-Filho RP. Study of the contralateral eye in patients with glaucoma and a unilateral perimetric defect. *J Glaucoma* 2000;9:34-37.
28. Mok KH, Lee VW, So KF. Retinal nerve fiber layer measurement by optical coherence tomography in glaucoma suspects with short-wavelength perimetry abnormalities. *J Glaucoma* 2003;12:45-49.
29. Sanchez-Galeana CA, Bowd C, Zangwill LM, et al. Short-wavelength automated perimetry results are correlated with optical coherence tomography retinal nerve fiber layer thickness measurements in glaucomatous eyes. *Ophthalmology* 2004;111:1866-1872.
30. Kanamori A, Nakamura M, Escano MF, et al. Evaluation of the glaucomatous damage on retinal nerve fiber layer thickness measured by optical coherence tomography. *Am J Ophthalmol* 2003;135:513-520.
31. Iester M, Broadway DC, Mikelberg FS, Drance SM. A comparison of healthy, ocular hypertensive, and glaucomatous optic disc topographic parameters. *J Glaucoma* 1997;6:363-370.

## PEER DISCUSSION

---

DR RICHARD P. MILLS: Investigation of technology that is capable of early detection of glaucomatous damage is impaired by the lack of a gold standard. Standard-of-care testing is simply too crude for early detection. Stretching the envelope for early detection requires an assumption that finding abnormalities in subjects at high risk for development of glaucomatous visual field loss that are not found in normal, low risk subjects is a form of validation for an early detection technology. Most such studies involve comparison of glaucoma suspects to normal individuals. Caprioli and coworkers focus on a subset of those suspect eyes: the perimetrically normal fellow eyes of patients with primary open angle glaucoma.

You want to exclude fellow eyes of patients with unilateral glaucoma, such as pseudoexfoliation or ICE syndrome, because the fellow eye is not at high risk. So the authors limited the study to patients with primary open angle glaucoma. It would have been even better if their subjects had no history of consistently different intraocular pressures in the two eyes that might have implied an unidentified cause for unilateral glaucoma.

Neither GDx nor OCT automatically control the centration of the optic disc in the image. Trained technicians do a reasonable job of this, but cannot do so consistently on serial images, since images are not registered by the software. Inferior NFL thickness was found by Caprioli to have the greatest area under the ROC curve, thereby indirectly validating its use as a detector of early glaucoma damage. However, the lack of registration of serial images impairs the use of this measure over time, to determine progression of damage. Consider the example of an image with the disc decentered down, in which the inferior NFL is sampled in the measurement ring very close to the disc margin, where it is thicker. On a subsequent image with the disc decentered up, the inferior NFL is sampled farther from the disc edge, giving the impression that it has become thinner. Such a conclusion is artifactual, based only on image centration.

These observations are not intended to be critical of the extraordinary quality of the paper you have just heard. Rather, they are intended to complement it.

DR JOSEPH CAPRIOLI: Let me amplify by saying that quantitative measurements sometimes give the illusion, because they are measurements and numbers, of reality or truth, when they are just as subject to error as our qualitative evaluations. Having said that, this is the first evidence that I have found that any of the quantitative approaches actually has the possibility of performing better than experienced clinicians evaluating optic disc photos. We should keep an open mind in this area. I have long been a proponent of using stereoscopic disc photos serially to detect early change in our patients. But better ways may become available in the future.